Available online at www.sciencedirect.com
ScienceDirect
Polymer 48 (2007) 7316–7328
polymer
www.elsevier.com/locate/polymer

Dynamic relaxation characteristics of crosslinked poly(ethylene oxide) copolymer networks: Influence of short chain pendant groups

Matthew A. Borns [a], Sumod Kalakkunnath [a,1], Douglass S. Kalika [a,*], Victor A. Kusuma [b], Benny D. Freeman [b]

[a] Department of Chemical and Materials Engineering and Center for Manufacturing, University of Kentucky, Lexington, KY 40506-0046, United States
[b] Center for Energy and Environmental Resources, Department of Chemical Engineering, University of Texas at Austin, Austin, TX 78758, United States

Received 5 July 2007; received in revised form 11 October 2007; accepted 17 October 2007
Available online 23 October 2007

Abstract

The dynamic relaxation characteristics of short-branch rubbery amorphous networks prepared by the photopolymerization of poly(ethylene glycol) diacrylate [PEGDA] crosslinker have been investigated using dynamic mechanical analysis and broadband dielectric spectroscopy. Copolymerization with low molecular weight acrylates was used to control effective crosslink density in the networks and led to the insertion of ethylene oxide pendant groups along the network backbone. Substantial differences in the sub-glass and glass–rubber relaxation properties of the copolymers were observed as a function of pendant length and the nature of the pendant terminal group (*e.g.*, −OH vs. $-OCH_3$); the results are compared with prior studies on model copolymers containing longer, more flexible side branches.

Keywords: Poly(ethylene oxide); Dynamic mechanical analysis; Dielectric spectroscopy

1. Introduction

The structure–property relationships that govern crosslinked polymer networks are a subject of intense interest from both a fundamental and a practical standpoint. Subtle changes in reaction conditions and composition can lead to substantial differences in network architecture and topology, resulting in significant variations in the thermomechanical performance properties of the material. In a recent series of papers, we have examined the molecular relaxation characteristics of a family of model rubbery poly(ethylene oxide) [PEO] networks based on the ultraviolet (UV) photopolymerization of poly(ethylene glycol) diacrylate [PEGDA] crosslinker [1–4]. These networks were intentionally formulated to enhance CO_2 solubility and diffusivity and show considerable promise for use as highly permeable CO_2-selective membranes appropriate for CO_2/H_2 and CO_2/CH_4 separations [5–9]. In the model networks, effective crosslink density was controlled stoichiometrically by copolymerization of the PEGDA crosslinker with mono-functional acrylates of similar chemical composition; *e.g.*, poly(ethylene glycol) methyl ether acrylate [PEGMEA] and poly(ethylene glycol) acrylate [PEGA]. The inclusion of mono-functional acrylate in the pre-polymerization mixture leads to the insertion of non-reactive, fixed-length pendant groups along the network backbone and a concomitant reduction in crosslink density (see schematics in Refs. [1,4]). For the model copolymers, the molecular weights of both the diacrylate crosslinker and the acrylate co-monomer were intentionally selected to achieve a constant chemical composition across each copolymer series, with the total ethylene oxide [EO] level maintained at approximately 82 wt%. This approach afforded the opportunity to investigate the influence of crosslink density

* Corresponding author. Department of Chemical and Materials Engineering and Center for Manufacturing, University of Kentucky, 177 Anderson Hall (Tower), Lexington, KY 40506-0046, United States. Tel.: +1 859 257 5507; fax: +1 859 323 1929.
E-mail address: kalika@engr.uky.edu (D.S. Kalika).
[1] Present address: ConocoPhillips Company, Bartlesville Technology Center, Bartlesville, OK 74004, United States.

0032-3861/$ - see front matter © 2007 Elsevier Ltd. All rights reserved.
doi:10.1016/j.polymer.2007.10.020

and branch content on the thermomechanical [1–4] and gas transport properties [6,7] of the networks essentially independent of changes in overall chemical constitution. Within this context, it was observed that relatively minor changes in network details, such as variations in the branch end group, had a strong impact on both the static and the dynamic properties of the polymers, as well as on their gas separation performance.

The influence of crosslink density on the glass–rubber and sub-glass relaxation characteristics of polymer networks has been reported for a wide range of material systems [10–29]. Dynamic thermal analysis techniques such as dynamic mechanical analysis (DMA) and broadband dielectric spectroscopy (BDS) have proven to be especially useful in providing detailed information regarding the intensity and time–temperature character of molecular relaxations in thermally stable polymer networks as a function of network architecture. A broad review of the various studies in the literature reveals that the glass–rubber relaxation characteristics of crosslinked polymer networks are highly sensitive to crosslink density and the nature and distribution of the crosslink junctions. The introduction of chemical crosslinks reduces molecular mobility and limits the segmental conformations that are accessible in the vicinity of the crosslink junctions. The resulting physical constraint is often manifested by an increase in the glass transition temperature (T_g) with increasing crosslink density, the effect being most pronounced at high crosslink densities where the average distance between crosslinks approaches the characteristic length scale required for cooperative segmental motion. In many network systems, including the model PEO networks described above, high degrees of crosslinking lead to an increase in the breadth of the glass–rubber relaxation owing to the increasingly heterogeneous motional environment experienced by the responding chain segments. Such heterogeneity may reflect both the proximity of a particular segment to an individual crosslink point and the potentially non-uniform distribution of crosslinks across the network. Further, increasing crosslink density often produces an enhancement in the fragility of the network [30]. Higher fragility values have been correlated with increased non-exponentiality of the glass–rubber response, behavior that is consistent with a greater degree of intermolecular cooperativity at higher extents of crosslinking [31].

Our previous studies on the PEGDA-based model copolymers established the viability of amorphous, rubbery crosslinked PEO networks as CO_2-selective gas separation membranes. The model copolymers, formulated so as to maintain a constant chemical composition, were based on the combination of PEGDA crosslink bridges comprising 14 ethylene oxide units and relatively long, flexible pendant branches (PEGMEA or PEGA) containing 7–8 ethylene oxide units. The distinguishing feature of the PEGMEA and PEGA comonomers was the branch end group ($-OCH_3$ vs. $-OH$), which led to important differences in the relaxation characteristics and gas transport properties of the networks. The inclusion of the methyl-terminated PEGMEA branches, for example, led to a systematic increase in fractional free volume (FFV) in the networks as compared to 100% crosslinked PEGDA, and a 5-fold increase in CO_2 permeability [1]. In an effort to further optimize the transport properties of this class of materials, new series of copolymers have been prepared using the PEGDA ($n = 14$) crosslinker in combination with ''short-branch'' co-monomers: ethylene glycol methyl ether acrylate [EGMEA], 2-hydroxyethyl acrylate [2-HEA], and diethylene glycol ethyl ether acrylate [DGEEA]. The chemical structures of the crosslinker and co-monomers are shown in Fig. 1. Specifically, we examine the influence of the short-branch acrylate co-monomers on the molecular relaxation characteristics of the networks as measured by dynamic mechanical analysis and broadband dielectric spectroscopy, with an ultimate goal of correlating the measured static and dynamic properties of these networks with their gas separation performance. The complementary nature of the dynamic mechanical and dielectric techniques allows for a full characterization of both the glass–rubber and the sub-glass relaxation processes operative in these networks and provides detailed insight as to how variations in network architecture affect the motional constraints that govern the relaxation properties of the materials. Such information is valuable both from a fundamental perspective and as applied to the design of membrane networks strategically formulated for specific gas separations.

2. Experimental

2.1. Materials

Poly(ethylene glycol) diacrylate [PEGDA; nominal MW = 700 g/mol] was obtained from Aldrich Chemical Company, Milwaukee, WI. The molecular weight and corresponding polydispersity of PEGDA were characterized using proton nuclear magnetic resonance (^{1}H NMR) and fast atom bombardment mass spectrometry (FAB-MS). These characterizations, which are detailed in previous publications, indicate a number-average molecular weight of 743 g/mol (NMR) for the crosslinker, consistent with a monomeric repeat value of $n \sim 14$ [1,6]. The acrylate co-monomers, ethylene glycol methyl ether acrylate [EGMEA; MW = 130 g/mol], 2-hydroxy ethyl acrylate [2-HEA; MW = 116 g/mol], and diethylene glycol ethyl ether acrylate [DGEEA; MW = 188 g/mol] were

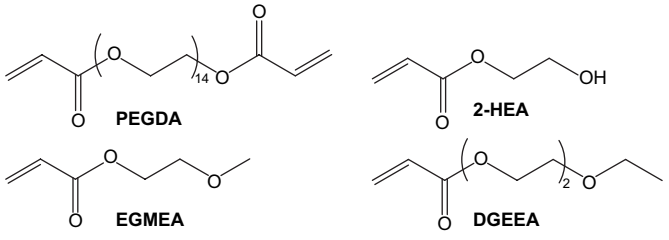

Fig. 1. Chemical structures of poly(ethylene glycol) diacrylate [PEGDA] crosslinker; ethylene glycol methyl ether acrylate [EGMEA], 2-hydroxyethyl acrylate [2-HEA], and diethylene glycol ethyl ether acrylate [DGEEA] co-monomers.

also obtained from Aldrich, as was 1-hydroxyl-cyclohexyl phenyl ketone [HCPK] photoinitiator. All reagents were used as received.

2.2. Copolymer film preparation

Copolymer films for dynamic mechanical and dielectric testing were prepared via UV photopolymerization; the film preparation method was the same as reported previously for the PEGDA/PEGMEA and PEGDA/PEGA copolymers [1]. Liquid pre-polymerization blends were formulated with the desired proportions of PEGDA crosslinker and acrylate co-monomer, as well as 0.1 wt% HCPK photoinitiator. The mixture was sandwiched between parallel quartz plates with controlled spacing and exposed to 312 nm UV light for 90 s at 3 mW/cm^2. Film thickness of the resulting crosslinked networks was ~1.0 mm for the dynamic mechanical specimens and ~0.35 mm for the dielectric samples; the precise thickness of each film was determined using a digital micrometer with precision to ±1 μm. Attenuated total reflection Fourier transform infrared spectroscopy (FTIR-ATR) was used to assess the degree of conversion of acrylate groups in the final films [6]. Across all three copolymer series, the incipient networks remained rubbery throughout the photopolymerization process ($T_g < 0$ °C), with essentially 100% conversion of the acrylate species observed.

2.3. Differential scanning calorimetry

Calorimetric glass transition temperatures were determined using a TA Instruments Q1000 differential scanning calorimeter (DSC) (New Castle, DE); the instrument was calibrated using an indium standard. Samples were initially quenched to −90 °C at a cooling rate of −5 °C/min, held for 5 min, and then scanned at a heating rate of 10 °C/min under a dry N_2 purge flow of 50 ml/min. The glass transition temperature was identified as the mid-point of the observed step change in heat capacity for each thermogram.

2.4. Dynamic mechanical analysis

Dynamic mechanical analysis was conducted using a Polymer Laboratories DMTA operating in single cantilever bending geometry. The specimen films had a thickness of 1.0 mm and were dried under vacuum at room temperature for at least 24 h prior to measurement; sample mounting procedures were designed to minimize exposure to ambient moisture. Storage modulus (E') and loss tangent (tan δ) were recorded at a heating rate of 1 °C/min with test frequencies of 0.1 Hz, 1 Hz, and 10 Hz. All measurements were carried out under an inert (N_2) atmosphere.

2.5. Dielectric relaxation spectroscopy

Dielectric spectroscopy was performed using the Novocontrol "Concept 40" broadband dielectric spectrometer (Hundsangen, Germany). Dielectric constant (ε') and loss (ε'') were recorded in the frequency domain (0.1 Hz to 1 MHz) at 4 °C isothermal intervals from −150 °C to 100 °C. In order to promote electrical contact during measurement, concentric silver electrodes were vacuum-evaporated on each polymer sample using a VEECO thermal evaporation system. Samples were subsequently mounted between gold platens and positioned in the Novocontrol Quatro Cryosystem. Each sample was dried under vacuum at room temperature prior to measurement; samples thickness was ~0.35 mm in all cases.

3. Results and discussion

3.1. Dynamic mechanical analysis

Dynamic mechanical results for crosslinked 100% PEGDA (XLPEGDA) and the PEGDA/EGMEA and PEGDA/2-HEA short-branch copolymer networks are plotted in Fig. 2 as storage modulus (E') vs. temperature at 1 Hz. The data show a step-wise drop in modulus that corresponds to the glass–rubber relaxation in these networks and which is accompanied by a peak in tan δ (not shown). The rubbery plateau modulus (E_R) displays a progressive decrease with increasing co-monomer content across each copolymer series, reflecting a reduction in effective crosslink density as governed by the stoichiometry

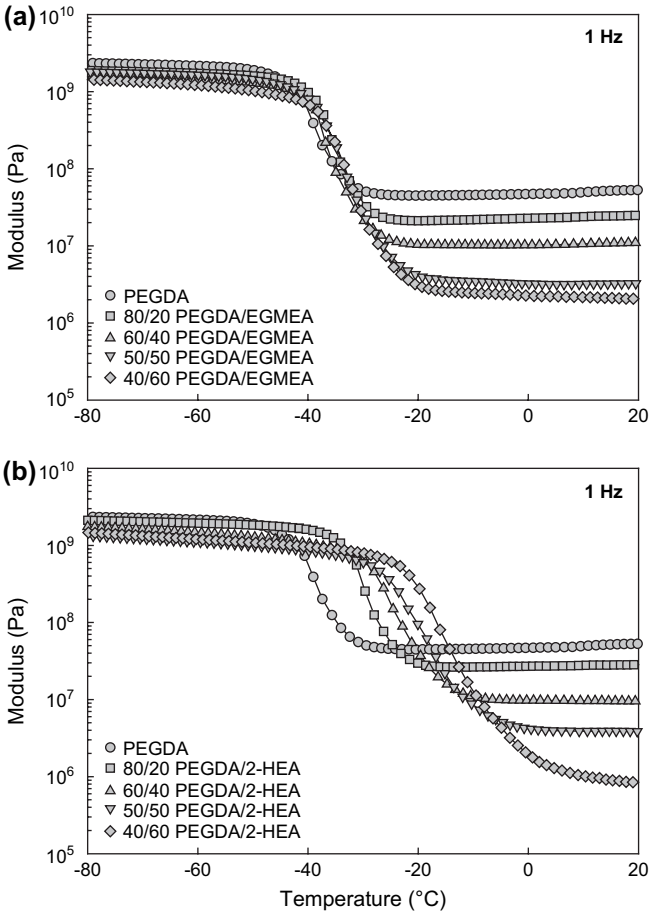

Fig. 2. Storage modulus (E'; Pa) vs. temperature (°C) at 1 Hz for PEGDA copolymer networks. (a) PEGDA/EGMEA; (b) PEGDA/2-HEA. All compositions are indicated on a wt% basis.

of the initial pre-polymerization reaction mixture. The dynamic mechanical transition temperature, T_α, defined as the tan δ peak temperature at a frequency of 1 Hz, is reported for each copolymer composition in Table 1.

Examination of the transition temperatures reported in Table 1 indicates that the inclusion of acrylate co-monomer influences the glass transition temperature of the copolymer networks to varying extents depending on the length of the pendants inserted along the network backbone and the nature of their end group. For the shortest pendants (*i.e.*, EGMEA and 2-HEA), which encompass only one ethylene oxide unit, the presence of the non-reactive side groups along the ($-CH_2CH_2-$) network backbone leads to an increase in glass transition temperature with increasing co-monomer content. Across the PEGDA/EGMEA series, T_α increases from −35 °C to −30 °C upon the inclusion of 60 wt% EGMEA co-monomer; this corresponds to a final molar composition of ~10% PEGDA and 90% EGMEA. The effect is more pronounced in the PEGDA/2-HEA series, where inclusion of the −OH terminated 2-HEA co-monomer produces an increase in T_α from −35 °C to −10 °C over the same composition range. For the PEGDA/DGEEA networks, however, which encompass longer pendants terminated by the $-OCH_2CH_3$ moiety, a small decrease in T_α is observed over the range of compositions tested. DSC scans completed on all three copolymer series reveal similar trends in T_g (see Table 1). The negative offset in T_g (DSC) vs. T_α (DMA) observed for most compositions reflects the longer experimental timescale associated with the calorimetric measurements; the calorimetric T_g value is typically correlated with a relaxation time of 100 s [30,31]. Representative DSC thermograms for the PEGDA/DGEEA series showing a progressive decrease in T_g with co-monomer content are presented in Fig. 3.

The results reported in Table 1 can be more readily understood when placed within the context of our previous model

Table 1
Characteristics of crosslinked PEGDA copolymer networks

	T_g^{DSC}	T_α (1 Hz)	β_{KWW}	FFV
XLPEGDA	−40	−35	0.30	0.118
PEGDA/EGMEA				
80/20	−36	−33	0.30	0.114
60/40	−35	−33	0.30	0.121
50/50	−35	−31	0.27	0.121
40/60	−34	−30	0.28	0.120
PEGDA/2-HEA				
80/20	−29	−27	0.28	0.103
60/40	−19	−20	0.25	0.098
50/50	−15	−15	0.23	0.094
40/60	−10	−10	0.20	0.092
PEGDA/DGEEA				
80/20	−41	−36	0.29	0.114
60/40	−44	−38	0.33	0.125
50/50	−46	−38	0.32	0.128

T_g (°C) corresponds to the calorimetric glass transition temperature; T_α (°C) is the dynamic mechanical peak temperature at 1 Hz; β_{KWW} is the Kohlrausch–Williams–Watts distribution parameter; FFV is the estimated fractional free volume based on bulk density measurements at 25 °C, see Ref. [7]. All copolymer compositions are reported on a wt% basis.

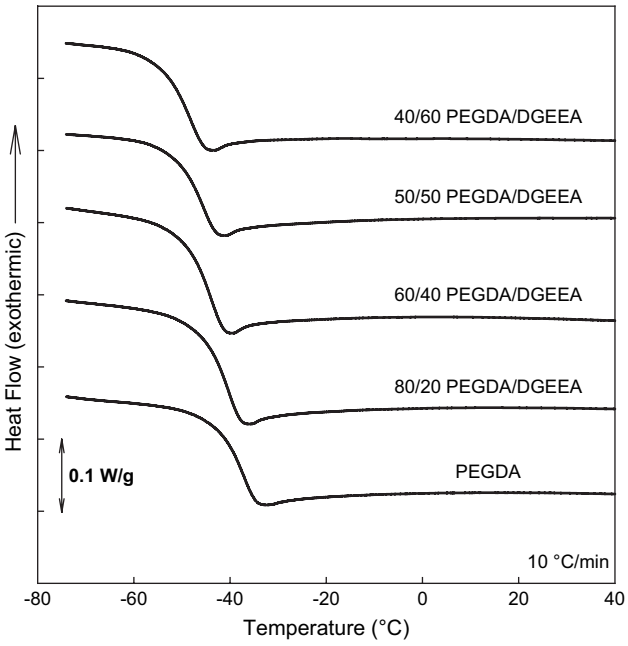

Fig. 3. Differential scanning calorimetric (DSC) thermograms for PEGDA/DGEEA copolymer networks; heating rate of 10 °C/min. The thermograms have been displaced vertically for clarity.

copolymer studies on PEGDA/PEGMEA and PEGDA/PEGA (see Refs. [1,7]). For the model networks, the introduction of PEGMEA or PEGA co-monomer resulted in the insertion of relatively long, flexible branches comprising 7–8 ethylene oxide repeat units along the network backbone. The presence of these long pendant chains, along with the accompanying reduction in effective crosslink density, led to a systematic decrease in measured glass transition temperature with increasing branch content. For the PEGDA/PEGMEA series, the $-OCH_3$ terminated pendants produced a decrease in calorimetric T_g of 27 °C as compared to XLPEGDA ($T_g = -40$ °C) over the full range of compositions studied, while the −OH terminated PEGA branches in the PEGDA/PEGA copolymers generated only a 5 °C depression in T_g [7]. The marked difference in the extent of T_g reduction across the two copolymer series was attributed to the possible formation of hydrogen bonds within the PEGDA/PEGA networks involving the −OH terminal group present on the PEGA branches. Such interactions have the potential to reduce local free volume and decrease segmental mobility within the network, leading to higher T_g values [32].

In the short-branch networks based on PEGDA/EGMEA and PEGDA/2-HEA, the introduction of backbone pendants containing only a single ethylene oxide segment appears to have a stiffening effect on the resulting copolymers, leading to a positive offset in the measured glass transition temperature despite a decrease in effective crosslink density. The stiffening effect is much stronger for the PEGDA/2-HEA series, where an increase in T_α of 25 °C is observed for samples containing 90 mol% 2-HEA. The origin of this behavior is again most likely the formation of hydrogen bonds involving the hydroxyl group present on the 2-HEA pendant. The

introduction of longer, non-interactive co-monomer chains (*e.g.*, DGEEA) along the network backbone leads to a reversal of the observed trend and a small decrease in T_g that is consistent both with the accompanying decrease in effective crosslink density and the classical depression in T_g observed for substituted vinyl polymers with increasingly longer flexible pendants [33].

Clearly, an important factor in determining the thermomechanical behavior of the PEGDA copolymer networks is the nature of the pendant terminal group. For networks containing −OH terminated pendants (*i.e.*, PEGDA/2-HEA, PEGDA/PEGA), hydrogen bonding appears to impose a significant constraint on the mobility of the polymer chain segments, leading to a substantial positive offset in T_g in the case of the PEGDA/2-HEA copolymers and otherwise diminishing the impact of the flexible branches across the PEGDA/PEGA series. The influence of the −OH terminated pendants is also evident in the static properties of these networks, specifically fractional free volume. Fractional free volume in the copolymer networks was estimated based on bulk density measurements conducted at 25 °C using a conventional density determination kit with *n*-hexane as the auxiliary liquid; see Ref. [7] for details. FFV values for the short-branch copolymer networks are reported in Table 1. For the PEGDA/2-HEA copolymer series, a decrease of ~20% in FFV is observed with increasing 2-HEA content that is consistent with a contraction of the polymer matrix owing to an increasing number of hydrogen bonds across the network. By contrast, for the PEGDA/DGEEA series, an overall increase in FFV of nearly 10% is realized with the introduction of slightly longer, non-interactive branches into the network. In the intermediate case (PEGDA/EGMEA), FFV remains approximately constant across the compositions studied. As noted above, FFV also increased in the PEGDA/PEGMEA model copolymers with increasing branch content, and this attribute proved decisive in the enhancement of CO_2 permeability that was observed for the PEGDA/PEGMEA series of membranes.

3.2. Time–temperature superposition

In addition to variations in the glass transition temperature, the copolymerization of PEGDA with mono-functional acrylates and the corresponding reduction in crosslink density can lead to changes in the breadth of the glass–rubber relaxation. The time–temperature superposition method has been used to construct master curves of storage (E') and loss (E'') moduli at constant temperature as a basis to evaluate the breadth of the glass transition [34]. Representative results for the 60/40 (wt%) PEGDA/EGMEA copolymer are shown in Fig. 4, with E' and E'' plotted vs. ωa_T. Here, ω is the applied test frequency ($\omega = 2\pi f$, with f expressed in Hz) and a_T is the dimensionless shift factor. The reference temperature ($T_{ref} = -40$ °C) was chosen based on the calorimetric glass transition temperature for XLPEGDA.

The glass–rubber relaxation data presented in Fig. 4 could be satisfactorily described using the Kohlrausch–Williams–Watts (KWW) stretched exponential relaxation time distribution function, with the breadth of the relaxation reflected in the KWW distribution parameter, β_{KWW}. β_{KWW} can range from 0 to 1: values approaching unity correspond to a narrow, single relaxation time (*i.e.*, debye) response, while lower values reflect greater relaxation breadth owing to greater intermolecular coupling and increased motional heterogeneity. The solid curves shown in Fig. 4 represent best fits to the KWW series approximations reported by Williams et al. [35].

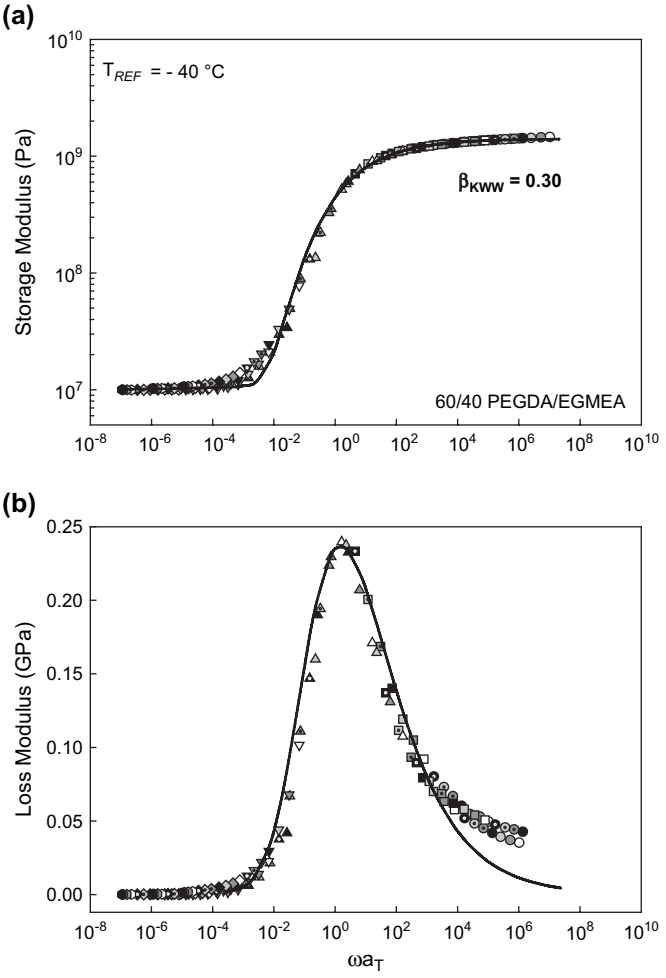

Fig. 4. Time–temperature master curves for 60/40 PEGDA/EGMEA network. (a) Storage modulus (Pa) vs. ωa_T; (b) Loss modulus (GPa) vs. ωa_T. $T_{ref} = -40$ °C; solid curve is KWW best fit. Various symbols correspond to discrete experimental temperatures across the range −60 °C to −10 °C.

Dynamic mechanical master curves and corresponding KWW curve fits for the PEGDA/EGMEA, PEGDA/2-HEA and PEGDA/DGEEA copolymer series are shown in Fig. 5. The relative positions of the curves along the horizontal (ωa_T) axis are consistent with the observed trends in T_α, with higher transition temperatures corresponding to a shift to the left (PEGDA/EGMEA; PEGDA/2-HEA), and lower transition temperatures corresponding to a shift to the right (PEGDA/DGEEA). The β_{KWW} value for each sample is reported in Table 1. Previous studies on the PEGDA/PEGMEA and PEGDA/PEGA flexible-branch networks indicated a gradual increase in β_{KWW} with increasing co-monomer content [1].

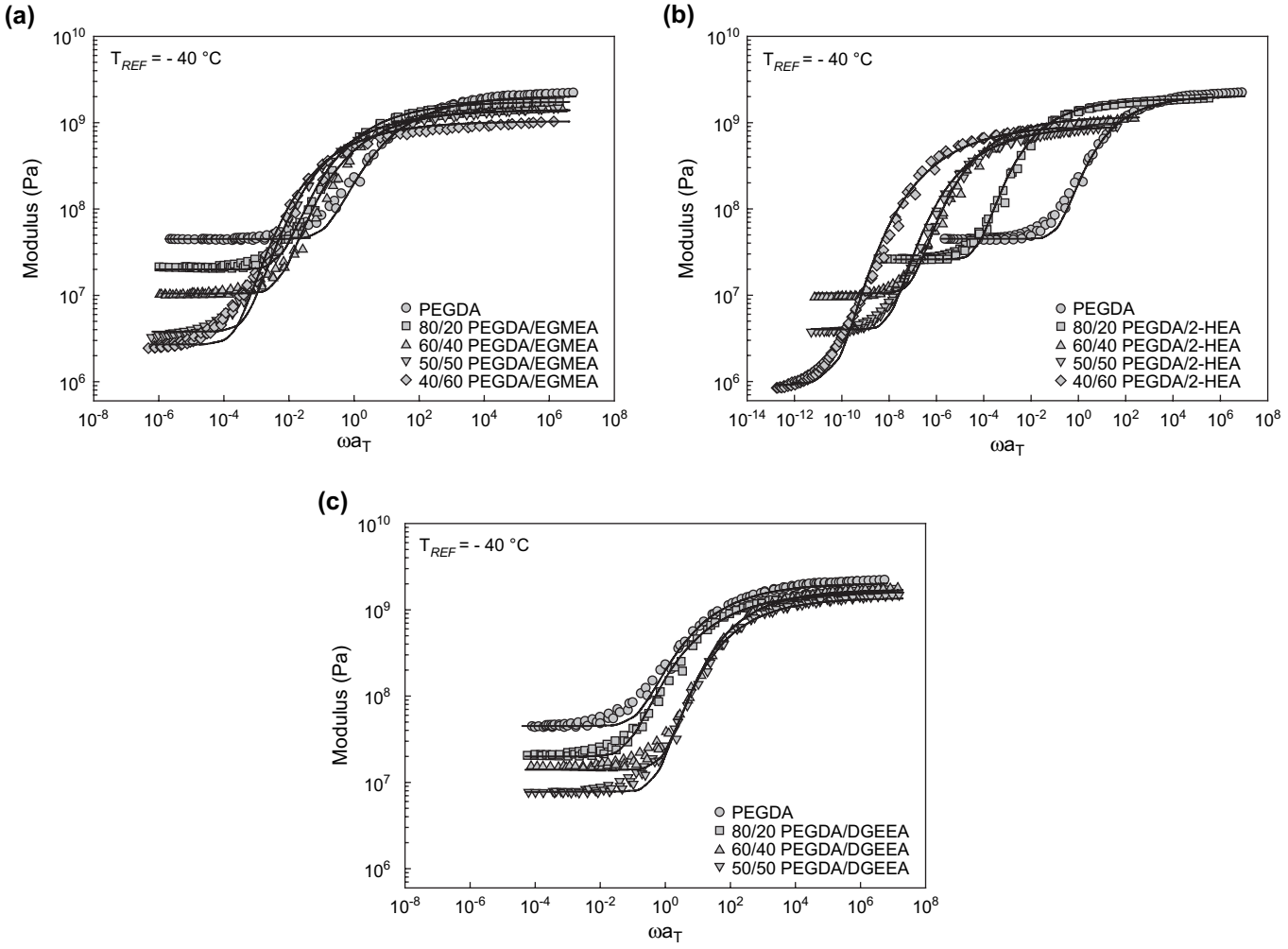

Fig. 5. Time–temperature master curves (storage modulus vs. ωa_T) for PEGDA copolymer networks. $T_{ref} = -40$ °C; solid curves are KWW best fits. (a) PEGDA/EGMEA; (b) PEGDA/2-HEA; (c) PEGDA/DGEEA.

This trend reflects a progressive narrowing of the glass–rubber relaxation with the introduction of flexible ethylene oxide branches and the accompanying reduction in effective crosslink density, and correlates with an overall decrease in the fragility of the crosslinked networks [31]. Relaxation narrowing is also evident to a small extent in the PEGDA/DGEEA copolymers, for which a slight increase in β_{KWW} is observed at lower crosslinker concentrations. However, in the case of the PEGDA/EGMEA and PEGDA/2-HEA series, the insertion of short ($n = 1$) ethylene oxide pendants along the network backbone leads to a broadening of the glass transition that is consistent with a greater degree of intermolecular cooperation within the segmental motions that constitute the glass transition. This effect is particularly strong for the PEGDA/2-HEA copolymers, where β_{KWW} drops from 0.30 (XLPEGDA) to 0.20 (40/60 wt% PEGDA/2-HEA). The introduction of the 2-HEA co-monomer leads to segmental dynamics that are more constrained and limited to a motional environment comprising lower free volume, despite the overall decrease in effective crosslink density that is achieved. The result is longer relaxation times and greater relaxation heterogeneity.

3.3. Dielectric relaxation spectroscopy

Dielectric relaxation spectroscopy serves as a valuable complement to dynamic mechanical analysis. Dielectric measurement techniques offer a number of advantages over DMA including a wide range of potential test frequencies and the ability to probe local dipolar motions that typically have only a weak influence on the bulk mechanical properties of the material. In this work, broadband dielectric spectroscopy (BDS) has been used to examine both the sub-glass and the glass–rubber relaxations that occur in the crosslinked PEO networks in an effort to elucidate the molecular origins associated with each relaxation and their relationship to network structure.

3.3.1. Sub-glass relaxations

A detailed study of the dielectric relaxation characteristics of crosslinked PEGDA has been reported in a prior publication [3]. XLPEGDA displays three distinct dielectric relaxation processes with increasing temperature: two sub-glass processes (designated as β_1 and β_2, respectively) and the glass–

rubber relaxation (designated as the α process). The dielectric relaxations detected in XLPEGDA exhibit very similar characteristics to those observed for crystalline PEO [3,36], and have been assigned to a highly localized process involving limited ethylene oxide motions (β_1), a "fast" segmental process with non-cooperative character that originates in the vicinity of the crosslink junctions in XLPEGDA and near the crystal–amorphous interface in PEO (β_2), and the glass–rubber (α) relaxation. BDS measurements conducted on the PEGDA/PEGMEA and PEGDA/PEGA model copolymers were useful in establishing the origin of these relaxations in that the influence of network structure and crosslink density on dielectric response could be assessed independent of changes in the overall chemical composition [4]. In the PEGDA/PEGMEA copolymers, for example, the β_2 sub-glass process was surprisingly sensitive to overall crosslink density, showing a systematic drop in relaxation intensity at lower degrees of crosslinking. It was proposed that the β_2 relaxation was the result of a subset of segmental motions that emerge due to the constraints imposed by the crosslink junctions, constraints that confine segmental motion and limit the sizescale and cooperativity of the dipolar response. Owing to the confined character and limited scale of these motions, the relaxation appears at a lower temperature (*i.e.*, shorter time) as compared to the glass–rubber process, and its overall intensity depends on the degree of constraint inherent to the network. As crosslink density decreases with copolymerization, the strength of the β_2 process diminishes. An analogy was drawn between the β_2 process of the networks and comparable relaxations observed not only in crystalline PEO but also within the confined layers of intercalated nanocomposites [37].

Fig. 6 presents dielectric loss measurements (ε'' vs. frequency) for the PEGDA/EGMEA and PEGDA/2-HEA short-branch copolymer networks recorded in the mid-range of the sub-glass relaxation region (−78 °C). For all compositions, the data show two overlapping relaxations, with the lower-temperature β_1 relaxation positioned on the high frequency side of the spectrum and the higher-temperature β_2 relaxation located at lower frequencies. The characteristics of the individual relaxations were determined in the frequency domain by fitting the data to a dual Havriliak–Negami (HN) expression [38,39]:

$$\varepsilon^* = \varepsilon' - i\varepsilon'' = \varepsilon_{U_1} + \sum_{i=1}^{2} \frac{\varepsilon_{R_i} - \varepsilon_{U_i}}{\left[1 + (i\omega\tau_{HN_i})^{a_i}\right]^{b_i}} \quad (1)$$

where ε_R and ε_U represent the relaxed ($\omega \to 0$) and unrelaxed ($\omega \to \infty$) values of the dielectric constant for each individual relaxation, $\omega = 2\pi f$ is the frequency, τ_{HN} is the relaxation time for each process, and a and b represent the broadening and skewing parameters, respectively. All HN fits presented here were obtained using the WinFIT software package provided with the Novocontrol spectrometer. In the case of the sub-glass relaxations (β_1 and β_2), it was possible to obtain satisfactory fits to the dielectric dispersions with the skewing parameter (b) set equal to 1; this corresponds to the Cole–Cole form of Eq. (1) [40]. Best fits to the dual model at −78 °C are shown as the solid curves in Fig. 6.

Inspection of the dielectric loss curves for the PEGDA/EGMEA and PEGDA/2-HEA copolymers reveals minimal variation in the peak positions (f_{MAX}) of the individual sub-glass relaxations relative to 100% crosslinked PEGDA, suggesting that the underlying molecular origins associated with these relaxations are unchanged upon the introduction of acrylate co-monomer. There is a marked contrast, however, in the relaxation intensity trends evident across the two copolymer data sets: for PEGDA/EGMEA, the intensities of the β_1 and β_2 sub-glass relaxations are almost independent of composition, while across the PEGDA/2-HEA series, there is a strong increase in relaxation intensity with increasing 2-HEA co-monomer content driven primarily by an increase in the strength of the β_2 process. As noted above, dielectric studies on the model copolymers have demonstrated a sensitivity of the β_2 relaxation to the degree of constraint inherent in the network, with decreasing crosslink density correlating with a reduction in β_2 relaxation strength. A similar effect is encountered in the results for the PEGDA/EGMEA copolymers, where the addition of EGMEA co-monomer leads to a small decrease in β_2 relaxation intensity, both in absolute terms and relative to the β_1 relaxation peak (see Fig. 6). In the PEGDA/2-HEA copolymers, however, the additional dipolar response associated with the −OH terminal group on 2-HEA is responsible for a dramatic increase in β_2 relaxation intensity.

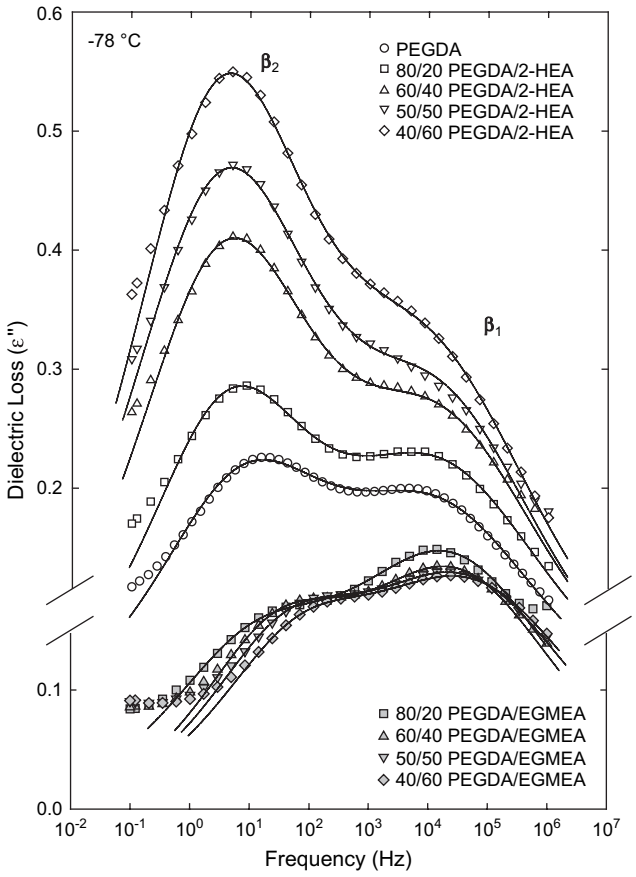

Fig. 6. Dielectric loss (ε'') vs. frequency for PEGDA/EGMEA and PEGDA/2-HEA copolymer networks at −78 °C. Solid curves are dual HN fits. Vertical axis break is provided for clarity.

This latter result underscores the sensitivity of the β_2 relaxation to the nature of the backbone pendants and the close correlation of the β_2 process to local pendant group motion in the short-branch networks. When longer hydroxyl-terminated branches are inserted within the network (*e.g.*, PEGDA/PEGA containing 7 EO linkages; see Ref. [4]), the relative dilution of the −OH dipole, as well as the uncoupling imparted by the flexible PEGA chain, reduces this effect considerably.

A distinctive feature of the β_2 process in the amorphous PEO networks is the variation of relaxation breadth as a function of temperature. For symmetric dispersions described by the Cole–Cole form of Eq. (1), breadth is quantified by the exponent "*a*". Values of the broadening parameter range from 0 to 1, with $a = 1$ corresponding to the ideal debye case and lower values of *a* reflecting broader relaxations. Results from the HN dual curve fits for PEGDA/2-HEA are shown in Fig. 7. Across the sub-glass transition region, the β_1 relaxation is observed to narrow with increasing temperature, reflecting a tighter distribution of relaxation times with increasing thermal energy; this result is consistent with the behavior observed for sub-glass and glass–rubber transitions in many flexible polymers [41]. The β_2 relaxation, however, broadens with increasing temperature, an outcome that reflects the confined character of the β_2 motions and their sensitivity to crosslink constraint. Runt and co-workers encountered the same trend for the intermediate sub-glass dispersion detected in crystalline PEO (designated γ'). They attributed the broadening to increasing "environmental asymmetry" between the crystal phase, which remains immobile, and the interlamellar amorphous phase, which becomes progressively more mobile with increasing temperature [36]. The enhanced asymmetry across the crystal–amorphous interface is consequently manifested by an increase in relaxation breadth at higher temperatures. A similar mechanism has been proposed for the β_2 relaxation in XLPEGDA [3], with the chemical crosslinks creating an apparent discontinuity in local mobility. For the PEGDA/2-HEA networks, the data in Fig. 7 show that the broadening effect persists even at substantially lower degrees of crosslinking. This same trend was observed for the model copolymers, as reported previously [4].

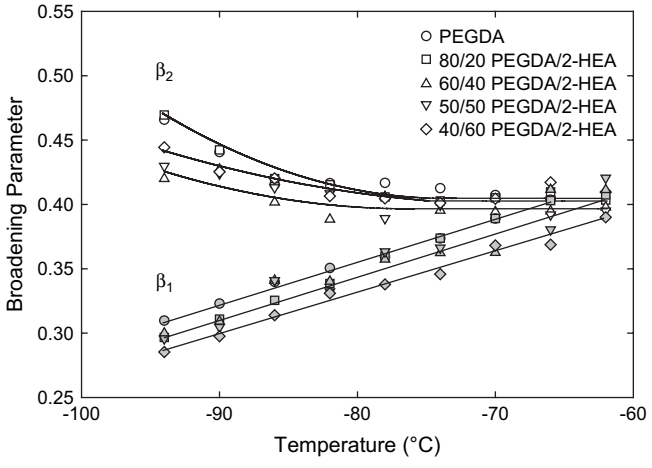

Fig. 7. Havriliak–Negami [HN] broadening parameter ($a_i \pm 0.01$) vs. temperature for PEGDA/2-HEA copolymer networks; see Eq. (1). β_1 [shaded symbols] and β_2 [unfilled symbols] sub-glass transitions. Solid curves are provided as a guide for the eye.

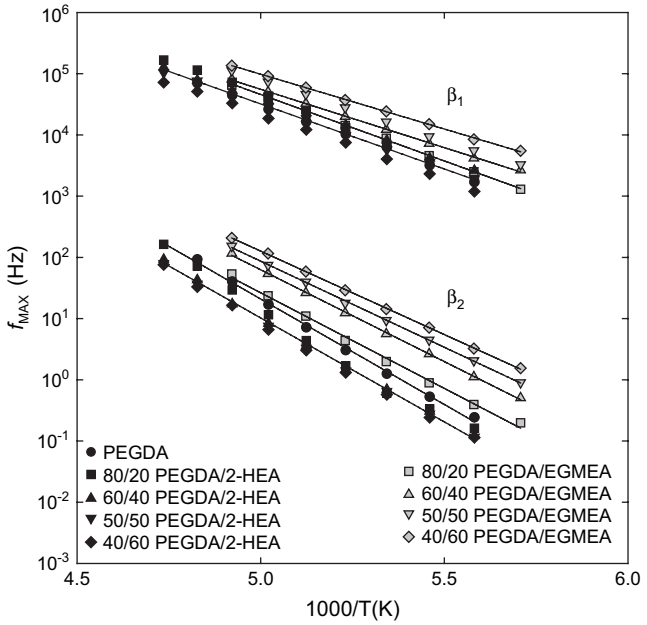

Fig. 8. Arrhenius plot of f_{MAX} (Hz) vs. 1000/*T* (K) for PEGDA/EGMEA and PEGDA/2-HEA copolymer networks; β_1 and β_2 sub-glass transitions. Solid lines are best fits to the Arrhenius expression.

The time–temperature relationships for the sub-glass relaxations in the short-branch copolymer networks are presented as Arrhenius plots of $\log(f_{MAX})$ vs. 1000/*T* (K) in Fig. 8. At each temperature, the peak maxima for the β_1 and β_2 relaxations were established from the dual HN curve fits with the skewing parameter, *b*, equal to 1 in all cases. The data obey a linear Arrhenius relationship for the various copolymers which is indicative of a localized, non-cooperative process for both sub-glass relaxations. Comparison with the results for XLPEGDA indicates very little difference in the apparent activation energy associated with each relaxation: $E_A(\beta_1) \sim 41$ kJ/mol and $E_A(\beta_2) \sim 65$ kJ/mol [3]. The relaxation peak positions associated with the β_1 and β_2 processes are nearly independent of composition in the PEGDA/2-HEA copolymers. For the PEGDA/EGMEA series, the sub-glass relaxation peaks shift to higher frequencies (or lower temperatures) with increasing co-monomer content, a trend that is apparent within the source data presented in Fig. 6.

3.3.2. Glass–rubber relaxation

Dielectric loss data measured in the glass–rubber relaxation region for the PEGDA/EGMEA, PEGDA/2-HEA and PEGDA/DGEEA copolymers are presented in Fig. 9. For the PEGDA/EGMEA and PEGDA/DGEEA series, the variation in T_g with copolymer composition is relatively small and the glass–rubber (α) and merged sub-glass (β) relaxation behaviors are well-represented by data sets collected at −30 °C (see Fig. 9a and c). Across the PEGDA/2-HEA series, T_g shifts much more strongly with composition, and the relaxation

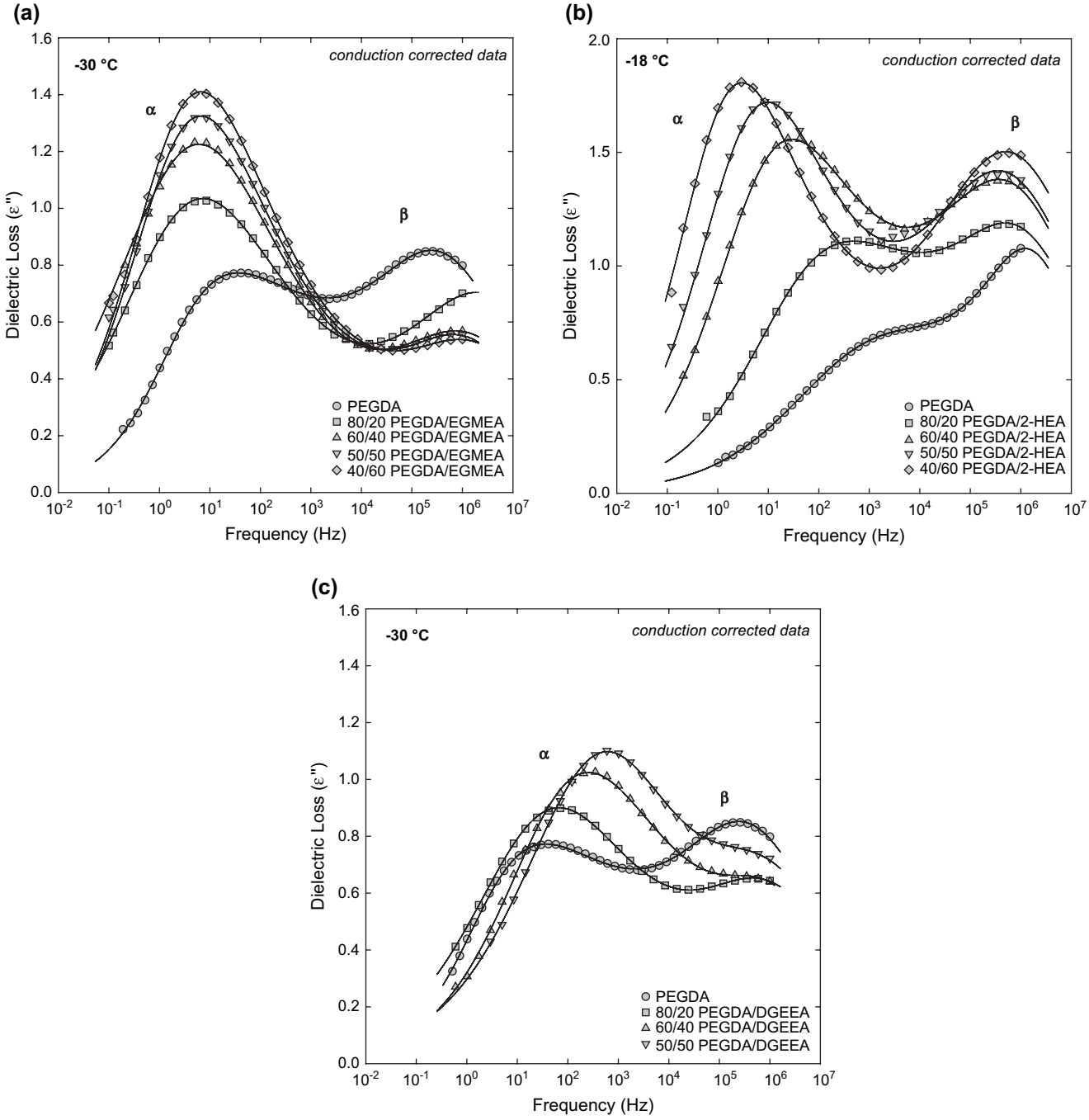

Fig. 9. Dielectric loss (ε'') vs. frequency for PEGDA copolymer networks in the vicinity of the glass transition. Data are corrected for conduction according to Eq. (2); solid curves are dual HN fits. (a) PEGDA/EGMEA (−30 °C); (b) PEGDA/2-HEA (−18 °C); (c) PEGDA/DGEEA (−30 °C).

trends are most effectively captured by a single plot at −18 °C (see Fig. 9b). The data presented in Fig. 9 have been analyzed using an expanded form of the HN equation in order to remove the influence of conduction:

$$\varepsilon^* = \varepsilon' - \mathrm{i}\varepsilon'' = \varepsilon_{\mathrm{U}_1} + \sum_{i=1}^{2} \frac{\varepsilon_{\mathrm{R}_i} - \varepsilon_{\mathrm{U}_1}}{\left[1 + (\mathrm{i}\omega\tau_{\mathrm{HN}_i})^{a_i}\right]^{b_i}} - \mathrm{i}\left(\frac{\sigma}{\varepsilon_{\mathrm{o}}\omega}\right) \qquad (2)$$

where σ is the conductivity and ε_{o} is the vacuum permittivity. The peak times (τ_{MAX}) associated with the individual relaxations were determined by the application of the dual HN model. For the merged β relaxation ($\beta_1 + \beta_2$), the skewing parameter (b) was always taken equal to 1, such that $\tau_{\mathrm{MAX}} = \tau_{\mathrm{HN}}$. Across the glass–rubber (α) relaxation, high-frequency skewing was observed, and the skewing parameter assumed values, $b < 1$. In this latter case, τ_{MAX} was determined directly from τ_{HN} and the values of the HN parameters, as described in Ref. [4].

Fig. 9 illustrates the combined influence of composition and effective crosslink density on copolymer dielectric relaxation response in the vicinity of the glass transition. Examination of the PEGDA/EGMEA results (Fig. 9a) reveals the

following features: (i) a modest shift in α relaxation peak position to lower frequencies upon the introduction of EGMEA co-monomer; (ii) a strong increase in α intensity with increasing co-monomer content; and (iii) a progressive decrease in β relaxation intensity with increasing EGMEA. The observed shift in α relaxation peak position to lower frequencies is equivalent to an upward shift in T_g for this series, and is consistent with the DSC and DMA results presented in Table 1. The increase in relaxation intensity associated with the α process could reflect not only loosening constraints across the network with decreasing crosslink density but also the change in chemical composition that occurs in the networks with increasing EGMEA content. As noted, the PEGDA/EGMEA and PEGDA/2-HEA series encompass molar compositions that range from 100% PEGDA crosslinker to ~10% crosslinker. The introduction of increasingly higher amounts of acrylate co-monomer leads to an increase in the relative proportion of −COO− ester dipoles within the network (dipole moment (μ) of approximately 1.8 D [42]), as compared to $-CH_2CH_2O-$ ethylene oxide dipoles ($\mu = 1.07$ D [43,44]). The increase in −COO− content, from roughly 12 mol% in XLPEGDA to 32 mol% in 40/60 PEGDA/EGMEA, appears to be the primary driving force behind the measured enhancement in α relaxation intensity.

The trends observed for the α relaxation in PEGDA/2-HEA are similar to those encountered with PEGDA/EGMEA. In the case of PEGDA/2-HEA (Fig. 9b), a greater shift in α peak position is evident reflecting the stronger positive offset in relaxation time (and corresponding T_g) that occurs with increasing 2-HEA branch content. The intensity of the α process scales with co-monomer content, as does the merged β process. Our analysis of the sub-glass relaxations at lower temperatures (−78 °C; see Fig. 6) indicates that changes in the intensity of the β process are due to the presence of terminal hydroxyls on the 2-HEA pendant groups, while the combined glass transition results for PEGDA/EGMEA and PEGDA/2-HEA suggest that the observed increase in the intensity of the α dispersion is due to an overall increase in −COO− ester dipoles within the network. This description also applies to the data for the PEGDA/DGEEA copolymers (*re:* Fig. 9c), which similarly show a progressive increase in dielectric α relaxation intensity with increasing co-monomer content. In addition, the PEGDA/DGEEA curves display a shift in the α relaxation peak to higher frequencies with increasing branch content that follows the decrease in glass−rubber relaxation temperature observed across this series.

The dielectric loss data recorded in the vicinity of the glass transition were analyzed according to Eq. (2) in order to subtract the conduction contribution and to determine the corresponding relaxation times (τ_{MAX}) and intensities ($\Delta\varepsilon = \varepsilon_R - \varepsilon_U$) associated with the individual relaxation processes. The time−temperature data for the α relaxation are plotted for each copolymer series according to Arrhenius form in Fig. 10, with $f_{MAX} = [2\pi\tau_{MAX}]^{-1}$. In general, the data display characteristics similar to those observed for XLPEGDA, and that are consistent with a process encompassing cooperative segmental reorientations. The results for the

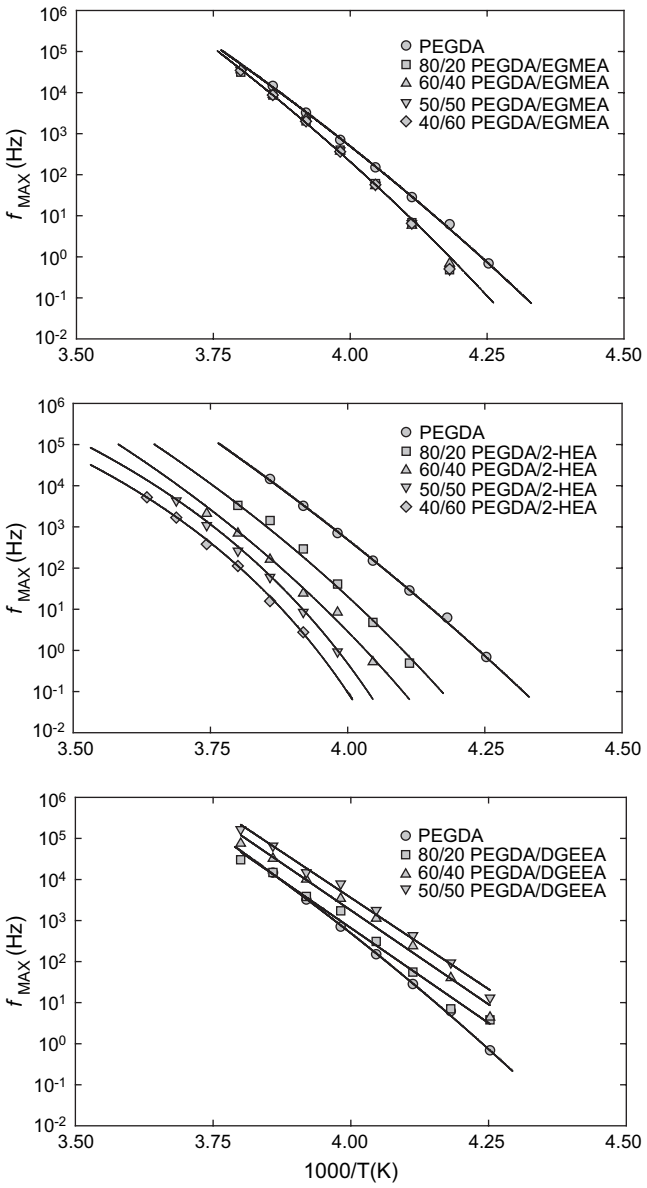

Fig. 10. Arrhenius plots of f_{MAX} (Hz) vs. 1000/T (K) for PEGDA/EGMEA, PEGDA/2-HEA and PEGDA/DGEEA copolymer networks; glass−rubber (α) relaxation. Solid curves are VFT fits.

PEGDA/EGMEA and PEGDA/2-HEA series can be described by the Vogel−Fulcher−Tammann (VFT) relation (see solid curves in Fig. 10), while the data for PEGDA/DGEEA display a more linear, Arrhenius character [45]. The relative positions of the curves along the reciprocal temperature axis match the trends in T_g indicated in Table 1.

The time−temperature characteristics of the glass−rubber (α) relaxation in the copolymers can be compared on a normalized basis by the construction of cooperativity or fragility plots, in which dimensionless relaxation time (τ/τ_α) is plotted vs. reciprocal temperature (T_α/T) [10,30]. In this case, T_α corresponds to the experimental temperature at which the relaxation time for the dielectric glass transition process, $\tau_\alpha = 1$ s. A combined cooperativity plot for the PEGDA/2-HEA and PEGDA/DGEEA copolymer series is presented in Fig. 11. Previous

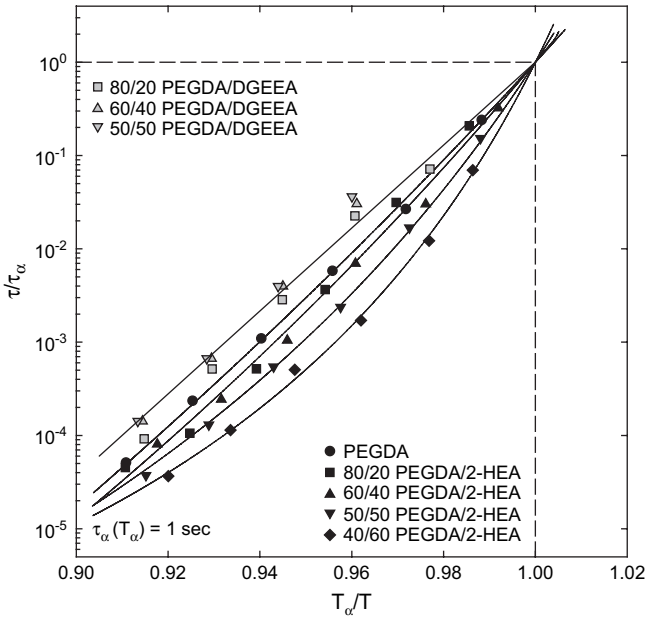

Fig. 11. Cooperativity plots of τ/τ_α vs. T_α/T for PEGDA/2-HEA and PEGDA/DGEEA copolymer networks; the relaxation time, $T_\alpha = 1$ s. Solid curves are VFT fits.

studies on the model copolymers [1], as well as on short-branch copolymer networks based on poly(propylene glycol) diacrylate crosslinker [4,46], has shown a reduced degree of time–temperature sensitivity and lower fragility at lower effective crosslink density. This same trend is evident in the PEGDA/DGEEA results plotted in Figs. 10 and 11, where the slope of the copolymer data is less than that observed for fully crosslinked XLPEGDA. Across the PEGDA/2-HEA copolymers, however, the opposite trend is evident, with network fragility increasing with increasing co-monomer content, indicating a higher apparent activation energy associated with the segmental motions inherent to the glass transition. The heightened fragility of the PEGDA/2-HEA copolymers presumably reflects a more constrained relaxation environment within the network, as manifested by the observed decrease in fractional free volume with increasing branch content. Bohmer et al. have reported a broad correlation between the fragility of a wide array of glass formers and the width of the glass–rubber relaxation, as expressed by the KWW distribution parameter [31]. Although the PEGDA/2-HEA and PEGDA/DGEEA networks display very different relaxation properties, their fragility characteristics are consistent with the Bohmer correlation. In the case of PEGDA/2-HEA, increasing branch content leads to greater network fragility and an increase in relaxation breadth (see β_{KWW} values from the dynamic mechanical studies in Table 1). For PEGDA/DGEEA, an overall decrease in fragility is observed with the insertion of the co-monomer branch groups, and this correlates with a small degree of relaxation narrowing.

A feature common to all three dielectric data sets reported in Fig. 9 is the progressive enhancement in glass–rubber (α) relaxation intensity that is evident with increasing co-monomer (*i.e.*, acrylate) content, an enhancement apparently due to the increasing overall dipolar character of the networks.

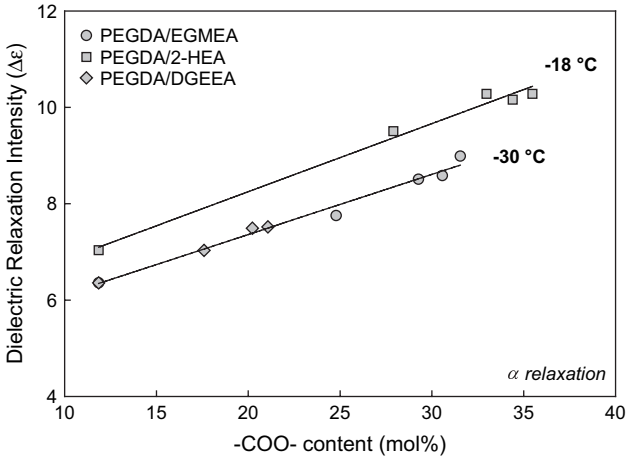

Fig. 12. Dielectric relaxation intensity ($\Delta\varepsilon$) vs. –COO– ester content in PEGDA copolymers at the temperatures indicated; glass–rubber (α) relaxation.

Fig. 12 shows the dielectric relaxation intensity of the α process ($\Delta\varepsilon_\alpha$) plotted against –COO– ester content for the three copolymer series studied here; the selected temperatures correspond to the curves presented in Fig. 9 and reflect conditions where deconvolution of the overlapping α and β relaxations can be reliably obtained across the full range of copolymer compositions. The data show a direct linear relationship between relaxation intensity and ester dipole content that is otherwise independent of the nature of the acrylate branch groups. This result for the α process stands in sharp contrast to the behavior observed for the sub-glass relaxations, where dielectric relaxation intensity correlates closely with the nature of the short-branch terminal group (*i.e.*, –OH vs. $-OCH_3$), but shows relatively little dependence on the overall ester content. In the case of the PEGDA/2-HEA networks, the –OH terminal group present on the branches appears to drive the increase in sub-glass relaxation intensity in a manner that may or may not reflect an additional contribution from the increasing number of ester dipoles present along the network backbone. For the PEGDA/EGMEA and PEGDA/DGEEA networks, two competing factors could be influencing the observed trend in dielectric intensity with increasing co-monomer content: decreasing crosslink density and reduced network constraint tend to produce a diminished sub-glass response (*re:* PEGDA/PEGMEA model networks [4]), while an increasing number of ester dipoles may enhance the measured dielectric loss. The net result is a modest decrease in the intensity of the merged β relaxation with increasing co-monomer content in PEGDA/EGMEA and PEGDA/DGEEA, as seen in Fig. 9.

4. Conclusions

The influence of composition and crosslink density on the relaxation behavior of short-branch PEO copolymer networks has been assessed using dynamic mechanical and dielectric methods. The networks were photopolymerized from mixtures of poly(ethylene glycol) diacrylate crosslinker ($n = 14$) and low molecular weight ethylene oxide acrylates. The inclusion of the mono-functional acrylates in the reaction mixture led to

the insertion of short-branch pendants along the network backbone and provided a mechanism to control crosslink density. The dynamic relaxation characteristics of the networks were strongly influenced by the presence of the backbone pendants and the nature of the pendant terminal group. Dynamic mechanical analysis indicated a progressive increase in the glass transition temperature of the networks with increasing branch content for the shortest pendants. The insertion of hydroxyl-terminated side groups via copolymerization with 2-HEA led to an especially strong positive offset in T_g owing to the formation of hydrogen bonds across the network and a corresponding decrease in fractional free volume. Time–temperature master curves showed an overall increase in dynamic mechanical relaxation breadth with increasing co-monomer content for the PEGDA/2-HEA copolymer series, even with the accompanying reduction in crosslink density. This result stood in contrast to the behavior of model copolymers containing more flexible side branches, for which relaxation narrowing is observed.

Dielectric studies on the short-branch copolymer series revealed a sensitivity to network architecture and dipolar constitution that was consistent with previous investigations on crystalline PEO, XLPEGDA and the model copolymers. The dielectric response across the sub-glass region displayed a direct correlation with the nature of the pendant end groups: inclusion of –OH terminated branches produced a dramatic increase in the strength of the sub-glass response due to the presence of the hydroxyl dipole, an effect that was absent for the copolymers containing methyl-terminated branches. The characteristics of the dielectric α process, which corresponded to the glass–rubber relaxation, reflected the influence of co-monomer content in a manner similar to the trends obtained via dynamic mechanical and calorimetric studies. For each of the three copolymer series examined, the dielectric relaxation peak time was observed to shift with composition according to the offsets measured in T_g, and the relaxation intensity correlated with the variations in ester dipole content that accompanied the overall changes in copolymer composition. Cooperativity plots based on the α dispersion data revealed a stronger time–temperature sensitivity for the PEGDA/2-HEA networks, indicating that these copolymers exhibit a more fragile character with increasing branch content, despite the concomitant decrease in crosslink density.

Acknowledgments

This work was supported in part by a grant from the Kentucky Science and Engineering Foundation as per Grant Agreement KSEF-148-502-05-130 with the Kentucky Science and Technology Corporation. In addition, we are pleased to acknowledge funding from the National Science Foundation Research Experiences for Undergraduates Program administered through the University of Kentucky Center of Membrane Sciences (DMR-0453488). Activities at the University of Texas were supported by the National Science Foundation under grant number CBET-0515425.

References

[1] Kalakkunnath S, Kalika DS, Lin H, Freeman BD. Macromolecules 2005;38:9679–87.
[2] Kalakkunnath S, Kalika DS, Lin H, Freeman BD. J Polym Sci Part B Polym Phys 2006;44:2058–70.
[3] Kalakkunnath S, Kalika DS, Lin H, Raharjo RD, Freeman BD. Polymer 2007;48:579–89.
[4] Kalakkunnath S, Kalika DS, Lin H, Raharjo RD, Freeman BD. Macromolecules 2007;40:2773–81.
[5] Lin H, Freeman BD. J Mol Struct 2005;739:57–74.
[6] Lin H, Kai T, Freeman BD, Kalakkunnath S, Kalika DS. Macromolecules 2005;38:8381–93.
[7] Lin H, Van Wagner E, Swinnea JS, Freeman BD, Pas SJ, Hill AJ, et al. J Membr Sci 2006;276:145–61.
[8] Lin H, Van Wagner E, Freeman BD, Toy LG, Gupta RP. Science 2006;311:639–42.
[9] Lin H, Van Wagner E, Raharjo R, Freeman BD, Roman I. Adv Mater 2006;18:39–44.
[10] Roland CM. Macromolecules 1994;27:4242–7.
[11] Roland CM, Ngai KL, Plazek DJ. Comput Theor Polym Sci 1997; 7:133–7.
[12] Schroeder MJ, Roland CM. Macromolecules 2002;35:2676–81.
[13] Glatz-Reichenbach JKW, Sorriero LJ, Fitzgerald JJ. Macromolecules 1994;27:1338–43.
[14] Fitz BD, Mijovic J. Macromolecules 1999;32:3518–27.
[15] Kannurpatti AR, Anderson KJ, Anseth JW, Bowman CN. J Polym Sci Part B Polym Phys 1997;35:2297–307.
[16] Kannurpatti AR, Anseth JW, Bowman CN. Polymer 1998;39:2507–13.
[17] Kannurpatti AR, Bowman CN. Macromolecules 1998;31:3311–6.
[18] Yu Kramarenko V, Ezquerra TA, Sics I, Balta-Calleja FJ. J Chem Phys 2000;113:447–52.
[19] Yu Kramarenko V, Ezquerra TA, Privalko VP. Phys Rev E 2001;64: 0518021–7.
[20] Yu Kramarenko V, Alig I, Privalko VP. J Macromol Sci Part B Phys 2005;44:697–709.
[21] Litvinov VM, Dias AA. Macromolecules 2001;34:4051–60.
[22] Alves NM, Gomez Ribelles JL, Gomez Tejedor JA, Mano JF. Macromolecules 2004;37:3735–44.
[23] Alves NM, Gomez Ribelles JL, Mano JF. Polymer 2005;46:491–504.
[24] Meseguer Duenas JM, Molina Mateo J, Gomez Ribelles JL. Polym Eng Sci 2005;45:1336–42.
[25] Viciosa MT, Rodrigues CM, Dionisio M. J Non-Cryst Solids 2005;351: 14–22.
[26] Viciosa MT, Rouze N, Dionisio M, Gomez Ribelles JL. Eur Polym J 2007;43:1516–29.
[27] Cook WD, Forsythe JS, Irawati N, Scott TF, Xia WZ. J Appl Polym Sci 2003;90:3753–66.
[28] Cook WD, Scott TF, Quay-Thevenon S, Forsythe JS. J Appl Polym Sci 2004;93:1348–59.
[29] Taheri Qazvini N, Mohammadi N. Polymer 2005;46:9088–96.
[30] Angell CA. J Non-Cryst Solids 1991;131–133:13–31.
[31] Bohmer R, Ngai KL, Angell CA, Plazek DJ. J Chem Phys 1993;99: 4201–9.
[32] Salmeron Sanchez M, Touze Y, Saiter A, Saiter JM, Gomez Ribelles JL. Colloid Polym Sci 2005;283:711–20.
[33] Shen MC, Eisenberg A. Prog Solid State Chem 1967;3:407–81.
[34] Ferry JD. Viscoelastic properties of polymers. 3rd ed. New York: John Wiley and Sons; 1980.
[35] Williams G, Watts DC, Dev SB, North AM. Trans Faraday Soc 1971;67: 1323–35.
[36] Jin X, Zhang S, Runt J. Polymer 2002;43:6247–54.
[37] Elmahdy MM, Chrissopoulou K, Afratis A, Floudas G, Anastasiadis S. Macromolecules 2006;39:5170–3.
[38] Havriliak S, Negami S. J Polym Sci Polym Symp 1966;14:99–103.
[39] Havriliak S, Havriliak SJ. Dielectric and mechanical relaxation in materials. Cincinnati: Hanser; 1997.

[40] Cole KS, Cole RH. J Chem Phys 1941;9:341–51.
[41] Schonhals A. Dielectric properties of amorphous polymers. In: Runt JP, Fitzgerald JJ, editors. Dielectric spectroscopy of polymeric materials: fundamentals and applications. Washington: American Chemical Society; 1997. p. 81–106.
[42] Saiz E, Hummel JP, Flory PJ, Plavsic M. J Phys Chem 1981;85: 3211–5.
[43] McClellan AL. Tables of experimental dipole moments, vol. 2. El Cerrito, CA: Rahara Enterprises; 1974.
[44] Diaz-Calleja R, Riande E. Calculation of dipole moments and correlation parameters. In: Runt JP, Fitzgerald JJ, editors. Dielectric spectroscopy of polymeric materials. Washington, DC: American Chemical Society; 1997. p. 139–73.
[45] Kremer F, Schonhals A. The scaling of the dynamics of glasses and supercooled liquids. In: Kremer F, Schonhals A, editors. Broadband dielectric spectroscopy. Berlin: Springer-Verlag; 2003. p. 99–129.
[46] Raharjo RD, Lin H, Sanders DF, Freeman BD, Kalakkunnath S, Kalika DS. J Membr Sci 2006;283:253–65.